

TABLE 3 Capacitance Matrix of a Coupled Line Structure

	C_{11}/ϵ_0	C_{12}/ϵ_0
This method	7.468	-0.936
[3]	6.868	-0.635
[9]	7.074	-0.664
[10]	7.123	-0.662

4. CONCLUSION

The calculation method presented herein is different from the one used in [3], as the upper and lower charges are directly evaluated without going through fictitious dielectric interfaces around the metal strips which induce more memory space and computational time. The involved matrix dimensions are independent of the number of dielectric interfaces, which inherently reduce the memory space and CPU time whenever the analysis presented in [3] is not a necessity. In addition to taking into account the anisotropy, which is very suitable for optoelectronic component analysis, the metal thickness does not have to be equal for different strips. The obtained recursive formula is very attractive for CAD tools used for multilayer multiconductor structures. It would be possible to extend this new approach to multilayer noncoplanar multiconductor structures.

REFERENCES

1. B. Toaquin, F. Medina, and M. Horno, *IEEE Trans Microwave Theory Tech* 45 (1997), 1619–1626.
2. H. Okazaki and T. Hirota, *IEEE Microwave Guided Wave Lett* 7 (1997), 1130–1132.
3. A. Papachristoforos, *Proc Inst Elect Eng* 141 (1994), 223–228.
4. G. Plaza, R. Marques, and V.K. Tripathi, *Microwave Opt Technol Lett* 2 (1990), 257–260.
5. R.T. Kollipara and V.K. Tripathi, *Microwave Opt Technol Lett* 3 (1990), 4–6.
6. H. Diestel, *AEU* 41 (1987), 169–175.
7. A.G. Keen, M.J. Walf, M.I. Sobhy, and A.J. Holden, *J Lightwave Technol* 8 (1990), 42–50.
8. T.N. Gang and C.H. Tan, *IEEE Trans Microwave Theory Tech* 38 (1990), 1130–1132.
9. C. Wei, R. Harrington, J. Mautz, and T. Sarkar, *IEEE Trans Microwave Theory Tech* MTT-32 (1984), 439–449.
10. W.T. Weeks, *IEEE Trans Microwave Theory Tech* MTT-18 (1970), 35–43.
11. C.J. Railton and J.P. McGeehan, *IEEE Trans Microwave Theory Tech* 38 (1990), 1017–1022.

© 2000 John Wiley & Sons, Inc.

SIMULATION OF MUTUAL COUPLING EFFECT IN CIRCULAR ARRAYS FOR DIRECTION-FINDING APPLICATIONS

Tao Su,¹ Kapil Dandekar,¹ and Hao Ling¹

¹Department of Electrical and Computer Engineering
University of Texas at Austin
Austin, Texas 78712-1084

Received 20 March 2000

ABSTRACT: The effect of mutual coupling on direction finding in circular arrays is simulated using rigorous electromagnetic computation

Contract grant sponsor: Office of Naval Research

Contract grant number: N00014-98-1-0178

Contract grant sponsor: Texas Higher Education Coordinating Board under the Texas Advanced Technology Program

and the MUSIC superresolution algorithm. The various scenarios studied include element spacing, noise level, antenna gain and delay, and platform effects. Our results show quantitatively the effect of mutual coupling on the direction-of-arrival estimates. The compensation of the coupling effect using the coupling matrix approach is also examined. This approach is found to be quite satisfactory in most cases, except when the array calibration data contain a high noise level or when strong platform effects are present. © 2000 John Wiley & Sons, Inc. *Microwave Opt Technol Lett* 26: 331–336, 2000.

Key words: array mutual coupling; direction-of-arrival estimates; compensation by coupling matrix

I. INTRODUCTION

It is well known that the mutual coupling between antenna elements in an array can strongly affect their radiation/receiving characteristics [1, 2]. For direction-finding applications, the direction-of-arrival estimates can be very sensitive to mutual coupling, and such effect needs to be properly accounted for [3]. An effective way to describe and compensate for the coupling effect in the array signal processing community is through the use of a coupling matrix [4]. It relates the active element patterns of the individual elements in the presence of the array environment to the idealized, free-standing element patterns. By measuring the actual array response at a few known incident angles during calibration, the coupling matrix can be estimated. Such an array calibration technique has been proven effective in many simulation and measurement results [5–7] involving simple antenna structures.

In this paper, we carry out a study to simulate the effect of mutual coupling for circular arrays. Our objectives are twofold. First, we set out to simulate the degradation effect due to mutual coupling in direction finding. Second, we set out to examine the validity of the coupling matrix model. This study is motivated by anomalies observed in measurement results from a smart antenna testbed for wireless communications [8]. Our approach is to use the full-wave electromagnetic solver NEC [9] to carry out the simulation. The superresolution algorithm MUSIC is applied to perform the direction-of-arrival (DOA) estimate. The various scenarios studied include element spacing, noise level, antenna gain and delay, and platform effects. Our results show quantitatively the effect of mutual coupling on DOA estimates. In addition, it is shown that the coupling matrix model is quite adequate under most scenarios examined by us.

II. FORMULATIONS FOR DIRECTION FINDING

The mutual coupling effect in an antenna array is commonly described in array signal processing by the following model [4]:

$$\mathbf{A}_{\text{true}} = \mathbf{C}\mathbf{A}_{\text{theo}} \quad (1)$$

where \mathbf{A}_{true} is the actual array response matrix, \mathbf{A}_{theo} is the ideal array response matrix in the absence of mutual coupling, and \mathbf{C} is an angular-independent coupling matrix. Each row of \mathbf{A}_{true} is the relative received signal strength of a particular antenna element as a function of the incident angle of an incoming plane wave. In the context of standard antenna terminology, this is known as the active element pattern of the array element. In the absence of mutual coupling, the receiving pattern for a single antenna element is independent of the others, and is only a function of the

incident angle and the position of the element. We consider the case where the sources as well as the array are located in the (x, y) -plane. Then the ideal element pattern can be written as

$$a_{\text{theo}, m}(\phi) = e^{jk(x_m \cos \phi + y_m \sin \phi)}, \quad m = 1, \dots, M \quad (2)$$

where M is the total number of elements, (x_m, y_m) are the coordinates of the m th element, and ϕ is the incident angle. The ideal array response is then

$$\mathbf{A}_{\text{theo}} = [a_{\text{theo}, 1}(\phi) a_{\text{theo}, 2}(\phi) \cdots a_{\text{theo}, M}(\phi)]^T. \quad (3)$$

Since \mathbf{A}_{theo} is known based on the array geometry, if \mathbf{A}_{true} is given, then \mathbf{C} can be determined by using the pseudoinverse concept as

$$\mathbf{C} = \mathbf{A}_{\text{true}} \mathbf{A}_{\text{theo}}^H (\mathbf{A}_{\text{theo}} \mathbf{A}_{\text{theo}}^H)^{-1}. \quad (4)$$

For simple antennas whose current distributions have the same shape but different amplitudes, \mathbf{C} can be found from \mathbf{A}_{true} at only a few observation angles. Once \mathbf{C} is known, \mathbf{A}_{true} can be interpolated to very fine angular granularity based on the model. Therefore, the coupling matrix concept is a very efficient description of the mutual coupling effect. We will use numerical simulation data to examine the validity of this model for direction finding.

To extract the directions of arrival from the received signals at the array, we use the superresolution algorithm MUSIC. If the signals come from N unknown directions, the received signal at the m th antenna can be written as

$$x_m(t) = \sum_{n=1}^N a_m(\phi_n) s_n(t) + z_m(t) \quad (5)$$

where $s_n(t)$ is the amplitude of the n th signal, $a_m(\phi_n)$ is the active element pattern of the m th element at the n th incident angle, and $z_m(t)$ represents the noise. Expressed in matrix form, (5) becomes

$$\mathbf{X} = \mathbf{A}\mathbf{S} + \mathbf{Z} \quad (6)$$

where \mathbf{A} is the array response. In principle, the actual array response \mathbf{A}_{true} should be used in (6) to properly model the received signal. However, if the ideal array response \mathbf{A}_{theo} is used instead, we, in effect, ignore the mutual coupling between the elements, and generate what we will call the uncompensated result. In the next section, we evaluate the performance difference between the compensated and uncompensated results to assess the significance of mutual coupling.

If the noise is assumed to be white Gaussian noise, the correlation matrix of \mathbf{X} can be separated into the signal part and the noise part:

$$\mathbf{R} = \mathbf{X}\mathbf{X}^H = \mathbf{A}\mathbf{S}\mathbf{S}^H\mathbf{A}^H + \sigma_n^2 \mathbf{I} \quad (7)$$

where σ_n^2 is the noise power. If the signals are uncorrelated, the N largest eigenvalues of \mathbf{R} correspond to the signal subspace, and the rest correspond to the noise subspace. Let \mathbf{V}_n denote the eigenvectors corresponding to the noise space.

The power spectrum defined in the MUSIC algorithm is then

$$P(\phi) = \frac{1}{\sum_{m=1}^M a_m^H(\phi) \mathbf{V}_n \mathbf{V}_n^H a_m(\phi)}. \quad (8)$$

The DOAs are determined by observing the peaks in the power spectrum as a function of incident angle.

III. SIMULATION RESULTS

A seven-element circular array shown in Figure 1 is used in the simulation. The radius of the circle is 0.5 wavelength. The array elements are half-wave dipoles. Each dipole is divided into 21 segments in the NEC simulation, with the load impedances equal to 73Ω at the center segments. First, the actual array response is computed densely from 0 to 360° in steps of 0.2° . This will be used to generate the reference DOA results. Next, we use the actual array response at eight incident angles equally spaced around a circle to determine the coupling matrix \mathbf{C} using (4). An interpolated version of the array response is then obtained using (1). The DOA results generated in this manner will be termed the ‘‘compensated-by-coupling matrix’’ (CC) results.

To illustrate the mutual coupling effect in direction finding, we first consider one incoming signal from the angle 0 , 45 , or 90° . The signal-to-noise ratio (SNR) is set to be 30 dB. The normalized MUSIC power spectra are plotted in Figure 2(a). The dashed curves are the uncompensated results computed using the ideal array response \mathbf{A}_{theo} . The solid curves are the reference results generated using the actual array response \mathbf{A}_{true} . The mutual coupling effect can be easily observed from the uncompensated curves where the peaks in the power spectra are significantly broadened. It is interesting to note that, due to the symmetry of the circular array structure, the direction of arrival is still estimated correctly by the uncompensated curve for a single incoming signal. However, as will be shown shortly, this will not be so when there is more than one incoming signal. We also test the validity of the coupling matrix model by generating the power spectra using the interpolated \mathbf{A}_{true} . The compensated-by-coupling matrix (CC) results nearly overlay the reference results, and are not shown. Only eight samples of the actual array response are used to generate the 7×7 coupling matrix. When compared to the densely computed actual array response of size 1800×7 , the coupling matrix model in (1) is indeed a very efficient representation of the mutual coupling effect. Figure 2(b) illustrates the power spectra when two

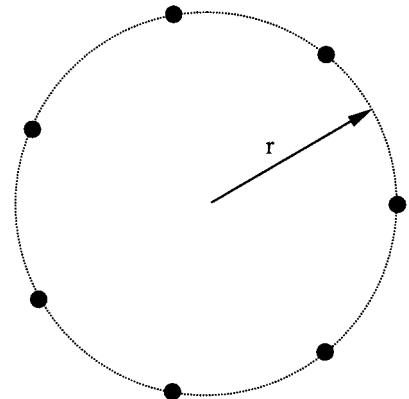
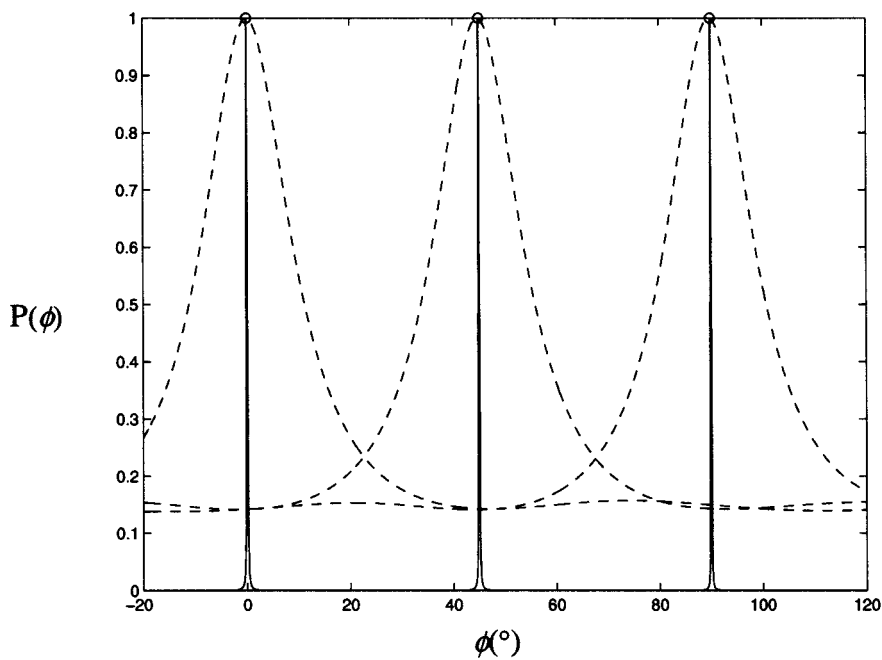
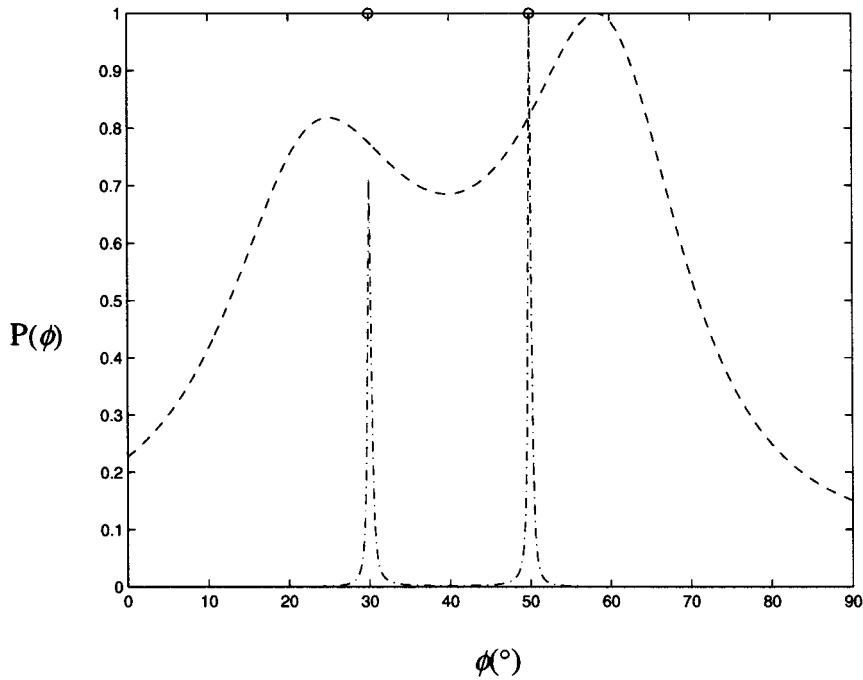


Figure 1 Circular array layout



(a)



(b)

Figure 2 MUSIC power spectrum before and after compensation of the mutual coupling effect. ---Uncompensated, -·-·- compensated by coupling matrix (CC), —reference. (a) Power spectrum with one incoming signal. (b) Power spectrum with two incoming signals

uncorrelated signals exist at 30 and 50°. The dashed curve is the uncompensated result, and the dash-dot curve is the CC result. When there is more than one signal, the coupling effect becomes more severe. The peaks of the uncompensated result no longer indicate the correct directions of arrival. However, the CC result still has sharp peaks at the correct DOA.

Next, we examine the mutual coupling effect when the spacing between array elements is reduced. We let the radius

of the circular array be 0.25 wavelength. The power spectra when there are two incoming signals at 30 and 50° are plotted in Figure 3. Compared with the previous example, we see that the mutual coupling effect is much stronger, as expected. The uncompensated curve, which ignores the mutual coupling, shows only one broad peak. The CC curve, on the other hand, still correctly resolves the two DOAs.

In the third example, we examine array calibration in a very noisy environment. We reduce the signal-to-noise ratio

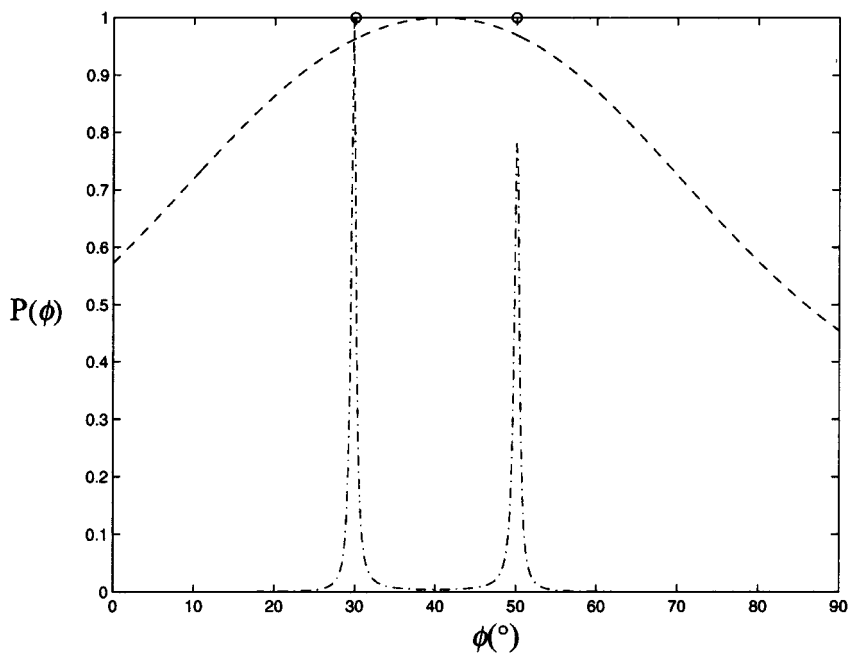


Figure 3 MUSIC power spectrum before and after compensation when the array spacing is halved. ---Un-compensated, ----CC

to 0 dB. Data used for both \mathbf{A}_{true} and \mathbf{C} contain white noise. Two signals are imposed on the array, and the MUSIC power spectra are plotted in Figure 4. The dashed curve is the un-compensated result, the dash-dot curve is the CC result, and the solid curve is the reference result. Since \mathbf{A}_{true} is collected in the presence of strong noise, the reference curve shows the degradation of the MUSIC algorithm due to noise. The CC curve includes the additional degradation from estimating the coupling matrix using noisy data. As we can see, when the coupling matrix is estimated in the noisy environ-

ment, the direction-finding result is not as satisfactory. The un-compensated result is again the poorest.

In the fourth example, we consider the antenna gain and delay difference between the array elements, in addition to the mutual coupling. We simulate this condition in NEC by using different load impedances for different antenna elements. The real and imaginary parts of the load impedances are randomly selected between -400 and 400Ω . The power spectra for one signal coming at 0 , 45 , or 90° are plotted in Figure 5. Some of the un-compensated results show false

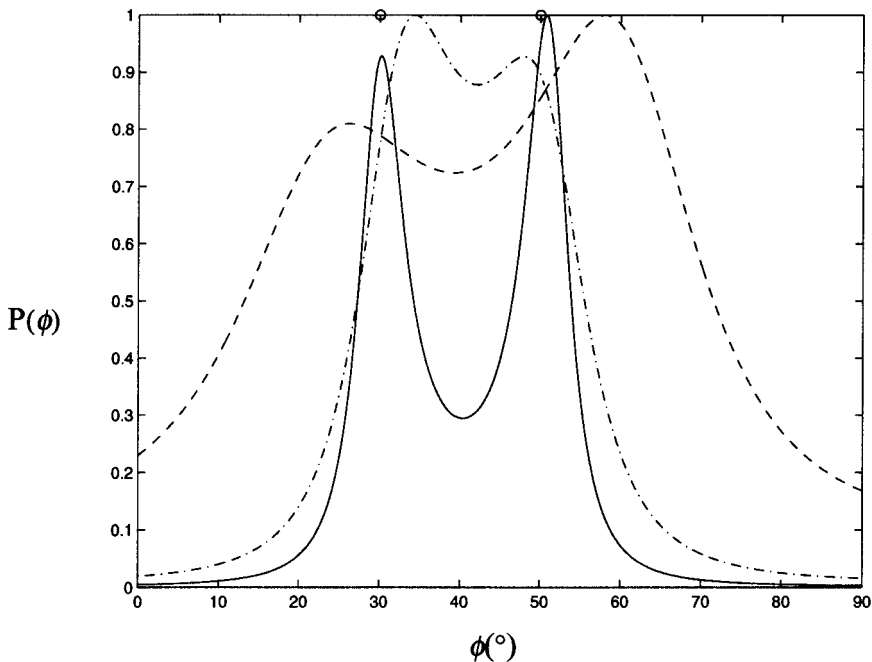


Figure 4 MUSIC power spectrum before and after compensation when the SNR is lowered to 0 dB. ---Un-compensated, ----CC, —reference

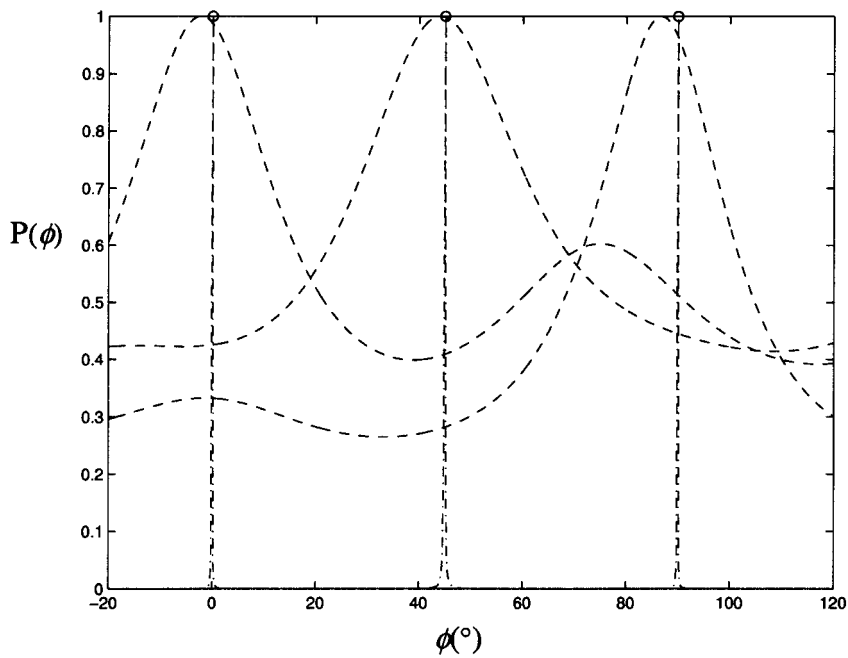


Figure 5 MUSIC power spectrum before and after compensation when unknown antenna gains and delays are considered. ---Uncompensated, -.-.-CC

peaks in the spectrum. The peaks corresponding to the correct DOAs also deviate from their correct locations. This implies that the error in antenna gain and delay is as significant as the mutual coupling effect. On the other hand, the sharp peaks from the CC results indicate that the gain and delay errors can still be correctly accounted for by the coupling matrix model. This is not surprising since the condition for (1) to be valid is still satisfied.

Finally, we consider an example where a platform structure is placed close to the array. We put a center conducting

post in the middle of the array to simulate a real antenna array layout. The post is 0.2 wavelength in radius, and is approximated by 36 vertical wires in NEC. We again consider the case of two incoming signals. The MUSIC power spectra are plotted in Figure 6, where the dashed curve is the uncompensated result, the dash-dot curve is the CC result, and the solid curve is the reference result. It can be observed that, although the CC result is much better than the uncompensated one, it cannot achieve the same resolution as the reference curve. This is because the actual array response is

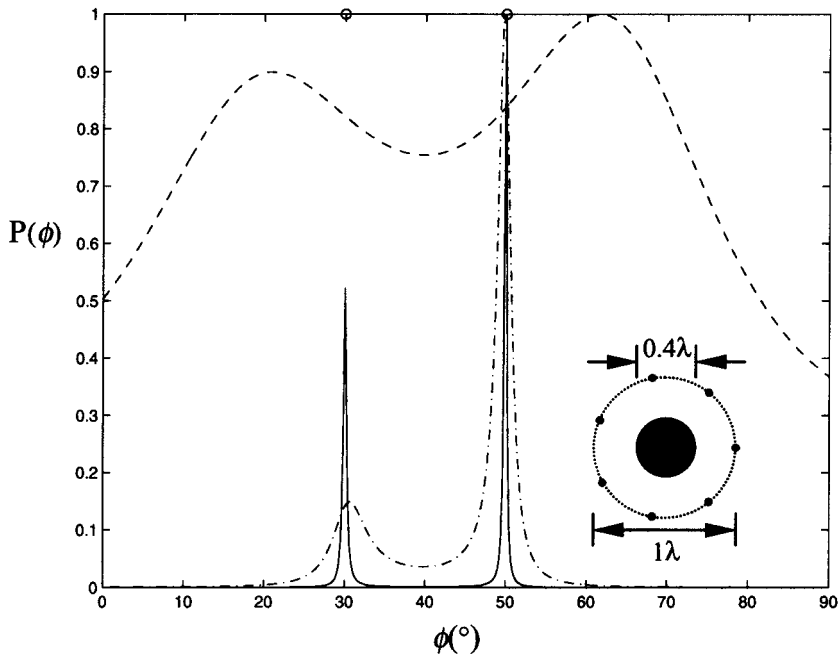


Figure 6 MUSIC power spectrum before and after compensation when the platform effect is considered. ---Uncompensated, -.-.-CC, —reference

not correctly modeled by (1), as the ideal element patterns used in (1) do not include the effect of the platform. Thus, the coupling matrix is no longer angular independent. However, if the two signals are not too closely spaced in angle, the DOA estimates are still satisfactory.

IV. CONCLUSIONS

In this paper, the effect of mutual coupling on direction-of-arrival estimates in a circular array is simulated using rigorous electromagnetic computation. The compensation of the coupling effect using the coupling matrix approach is also examined. Numerical results show that the mutual coupling effect can lead to significant errors in direction finding when not properly accounted for. The compensation of the mutual coupling effect using the coupling matrix approach is found to be quite satisfactory in most cases. The coupling matrix model provides a very sparse description of the array response. It can also take into account additional antenna gain and delay errors. However, the performance of this approach degrades in cases when the array calibration data contain a high noise level or when strong platform effects are present.

REFERENCES

1. D.F. Kelley and W.L. Stutzman, Array antenna pattern modeling methods that include mutual coupling effects, *IEEE Trans Antennas Propagat* 41 (1993), 1625–1632.
2. I.J. Gupta and A.A. Ksienski, Effect of mutual coupling on the performance of adaptive arrays, *IEEE Trans Antennas Propagat* AP-31 (1983), 785–791.
3. T. Svantesson, Modeling and estimation of mutual coupling in a uniform linear array of dipoles, *IEEE Int Conf Acoust, Speech, Signal Processing*, Phoenix, AZ, 1999, pp. 2961–2964.
4. B. Friedlander and A.J. Weiss, Direction finding in the presence of mutual coupling, *IEEE Trans Antennas Propagat* 39 (1991), 273–284.
5. C.M.S. See, A method for array calibration in parametric sensor array processing, *IEEE Singapore Int Conf Commun Sys*, Singapore, 1994, pp. 915–919.
6. J. Pierre and M. Kaveh, Experimental performance of calibration and direction-finding algorithms, *IEEE Int Conf Acoust, Speech, Signal Processing*, Toronto, Ont., Canada, 1991, pp. 1365–1368.
7. A.N. Lemma, E.F. Deprettere, and A.J. Veen, Experimental analysis of antenna coupling for high-resolution DOA estimation algorithms, *IEEE Workshop Signal Processing Advances in Wireless Commun*, Annapolis, MD, May 1999, pp. 362–365.
8. S.S. Jeng, G.T. Okamoto, G. Xu, H.P. Lin, and W.J. Vogel, Experimental evaluation of smart antenna system performance for wireless communications, *IEEE Trans Antennas Propagat* 46 (1998), 749–757.
9. NEC-2 manual, Lawrence Livermore National Lab, 1996.

© 2000 John Wiley & Sons, Inc.

MODELING OF THE VERTICAL PLANE PROPAGATION FOR MOBILE SATELLITE COMMUNICATIONS IN URBAN ENVIRONMENTS

Lorenzo Rubio¹ and Narcís Cardona¹

¹ Departamento de Comunicaciones
Polytechnic University of Valencia
Escuela Universitaria de Gandía
46730 Playa de Gandía, Valencia, Spain

Received 22 March 2000

ABSTRACT: This letter presents a characterization of the vertical plane propagation in terms of the satellite elevation angle for different mechanisms of propagation. The effect of blockage by buildings on the received signal level versus the satellite elevation angle at L-band for urban environments is performed using the uniform theory of diffraction (UTD). © 2000 John Wiley & Sons, Inc. *Microwave Opt Technol Lett* 26: 336–338, 2000.

Key words: satellite mobile communications; uniform theory of diffraction; radio-wave propagation

1. INTRODUCTION

In geostationary earth-orbit (GEO) systems, the satellite remains static related to the receiver position. Nevertheless, this does not occur in low earth-orbit (LEO) and medium earth-orbit (MEO) systems, where the satellite could be at any elevation angle. In this case, any multipath contribution which arrives at the receiver position comes from different propagation mechanisms (diffracting, reflecting, and scattering processes) which are closely related to the satellite elevation angle. The geometry of the propagation mechanisms is shown in Figure 1. The received signal at the mobile antenna is estimated for different satellite elevation angles (θ) from 0 to 90°. Depending on the satellite elevation angle, different ray contributions can reach the mobile receiver. Three different propagation regions are suggested in Figure 1 in order to study different propagation forms. These possible regions, and the contributions considered in each case, are formulated as follows.

- *Region 1* ($0^\circ \leq \theta \leq \theta_{12}$): We consider the multiple diffraction over buildings. The propagation losses in this case are obtained using the UTD formulation.
- *Region 2* ($\theta_{12} < \theta \leq \theta_{23}$): We consider only the final diffraction (diffraction at the upper edge of the nearest building to the receiver position).
- *Region 3* ($\theta_{23} < \theta \leq 90^\circ$): We consider the final diffraction and the free-space attenuation of the direct path.

This classification in regions does not consider the radiation pattern of the mobile antenna. An omnidirectional antenna in the elevation plane is assumed.

In many applications, digital information on the urban environment is available. In this situation, it is possible to consider real building height and the space between them. If digital information about the urban area is not available, the profile between the transmitter and receiver (vertical plane propagation) can be generated randomly, taking into account average buildings height and average building separation for different cities with similar characteristics. In this case, the building height can be modeled by a Gaussian distribution,